The NADPH-dependent thioredoxin system constitutes a functional backup for cytosolic glutathione reductase in *Arabidopsis*

Laurent Marty[a], Wafi Siala[b], Markus Schwarzländer[c], Mark D. Fricker[c], Markus Wirtz[a], Lee J. Sweetlove[c], Yves Meyer[b], Andreas J. Meyer[a,1], Jean-Philippe Reichheld[b], and Rüdiger Hell[a]

[a]Heidelberg Institute for Plant Science, Heidelberg University, Im Neuenheimer Feld 360, 69120 Heidelberg, Germany; [b]Laboratoire Génome et Développement des Plantes, Unité Mixte de Recherche 5096, Centre National de la Recherche Scientifique/UP-Institut de Recherche pour le Développement/Université de Perpignan 52, Avenue Paul Alduy, 66860 Perpignan Cedex, France; and [c]Department of Plant Sciences, University of Oxford, South Parks Road, Oxford OX1 3RB, United Kingdom

Edited by Bob B. Buchanan, University of California, Berkeley, CA, and approved April 10, 2009 (received for review January 8, 2009)

Tight control of cellular redox homeostasis is essential for protection against oxidative damage and for maintenance of normal metabolism as well as redox signaling events. Under oxidative stress conditions, the tripeptide glutathione can switch from its reduced form (GSH) to oxidized glutathione disulfide (GSSG), and thus, forms an important cellular redox buffer. GSSG is normally reduced to GSH by 2 glutathione reductase (GR) isoforms encoded in the *Arabidopsis* genome, cytosolic GR1 and GR2 dual-targeted to chloroplasts and mitochondria. Measurements of total GR activity in leaf extracts of wild-type and 2 *gr1* deletion mutants revealed that ≈65% of the total GR activity is attributed to GR1, whereas ≈35% is contributed by GR2. Despite the lack of a large share in total GR activity, *gr1* mutants do not show any informative phenotype, even under stress conditions, and thus, the physiological impact of GR1 remains obscure. To elucidate its role in plants, glutathione-specific redox-sensitive GFP was used to dynamically measure the glutathione redox potential (E_{GSH}) in the cytosol. Using this tool, it is shown that E_{GSH} in *gr1* mutants is significantly shifted toward more oxidizing conditions. Surprisingly, dynamic reduction of GSSG formed during induced oxidative stress in *gr1* mutants is still possible, although significantly delayed compared with wild-type plants. We infer that there is functional redundancy in this critical pathway. Integrated biochemical and genetic assays identify the NADPH-dependent thioredoxin system as a backup system for GR1. Deletion of both, NADPH-dependent thioredoxin reductase A and GR1, prevents survival due to a pollen lethal phenotype.

redox homeostasis | redox imaging | redox-sensitive GFP | thioredoxin reductase

Thiol-redox biochemistry is a common feature of life and is involved in a broad range of physiological and pathological processes. Thus, tight control of cellular redox homeostasis is essential for maintenance of normal metabolism and redox-dependent signaling. In general, several metabolic reactions and, to a larger extent, stress-induced processes lead to the formation of reactive oxygen species (ROS). The concomitant oxidation is buffered through a tight network of antioxidant enzymes and low-molecular weight antioxidants (1). The most prevalent non-protein thiol-based redox buffer is the tripeptide glutathione, which is present in low millimolar concentrations in most eukaryotic cells. Under nonstress conditions, cytosolic glutathione is present mainly in the reduced form (GSH) with only nanomolar concentrations of the oxidized form, glutathione disulfide (GSSG) (2, 3). In plants, ROS are at least partially detoxified through the glutathione-ascorbate-cycle at the expense of electrons from the GSH pool (4), causing a transient oxidation of the GSH pool. This transient change in glutathione redox potential (E_{GSH}) has been suggested to be part of signaling cascades leading to changes in gene expression during stress responses and developmental processes (5, 6). The transmission of such signals is likely to be facilitated by glutaredoxins (GRXs) (6), which equilibrate E_{GSH} with the redox potential of target protein thiols. Indeed, GRXs have been shown to be involved in disease resistance and developmental processes, suggesting that downstream events in these processes are modified by E_{GSH} (7, 8).

NADPH-dependent glutathione reductase (GR), a member of the FAD-binding disulfide reductase superfamily, is the major enzyme responsible for reduction of GSSG to GSH in most organisms, with only few GR-deficient exceptions (9, 10). The *Arabidopsis* genome contains 2 GR genes. One gene codes for an organellar isoform (GR2), which is dual-targeted to chloroplasts and mitochondria (11). GR2 is essential for plant development, which is evident from lethality of deletion mutants in early embryo development (12). The second gene codes for the cytosolic GR1. Expression analysis by scrutiny of the Genevestigator microarray database (13) shows *GR1* to be responsive to several stress factors. Although GR activity is one of the most frequently monitored enzyme activities after stress application, there is still very little information on the biochemical properties of *Arabidopsis* GR1. Because *gr1* deletion mutants have not been reported in plants, we questioned whether other oxidoreductases may provide a functional backup system for GR1 and, thus, conceal function on gene disruption (14).

Like GRs, NADPH-dependent thioredoxin reductases (NTRs) also belong to the FAD-binding disulfide reductase superfamily (15). In *Arabidopsis*, NADPH-dependent thioredoxin reductase A (NTRA) and NADPH-dependent thioredoxin reductase B (NTRB) result from recent gene duplication and constitute the major route to reduce mitochondrial and cytosolic thioredoxins (TRXs) (16, 17). Nevertheless, the double knockout *ntra ntrb* was found to be viable, although it was hypersensitive to depletion of the GSH pool (18). A different, although less efficient, reduction system consisting of GRX and TRX was apparently able to complement the NTR function (18). To be maintained in the reduced form, GRX requires GSH, GR, and NADPH as the primary electron donor. Partial redundancies between the NTR/TRX system and the GSH redox system have also been observed in *Escherichia coli* and *Saccharomyces cerevisiae* (19, 20). However, in fission yeast, GR is indispensable for growth under aerobic conditions (21).

Author contributions: L.M., M.D.F., A.J.M., J.-P.R., and R.H. designed research; L.M., W.S., and M.S. performed research; M.D.F. contributed new reagents/analytic tools; L.M., W.S., M.W., L.J.S., A.J.M., J.-P.R., and R.H. analyzed data; and L.M., M.D.F., Y.M., A.J.M., J.-P.R., and R.H. wrote the paper.

The authors declare no conflict of interest.

This article is a PNAS Direct Submission.

[1]To whom correspondence should be addressed. E-mail: ameyer@hip.uni-heidelberg.de.

This article contains supporting information online at www.pnas.org/cgi/content/full/0900206106/DCSupplemental.

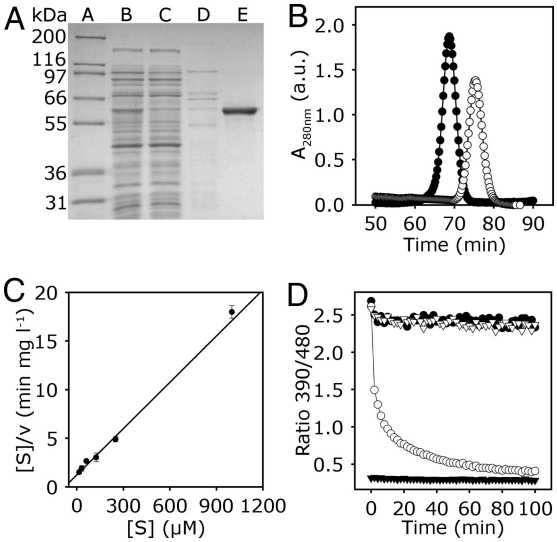

Fig. 1. Biochemical characterization of cytosolic GR1. (*A*) Expression and purification of GR1. SDS/PAGE Gel stained with Coomassie Blue. Lane A, molecular mass standard. Lanes B–E, purification of GR1 expressed in *E. coli* HMS 174 cells, as follows: 8 μg of crude extract (lane B); 8 μg of flow through after loading the crude extract on Ni^{2+}-NTA column (lane C); wash step with 80 mM imidazole (lane D); 2 μg of purified GR1 eluted with 150 mM imidazole (lane E). (*B*) Size exclusion chromatography of GR1 and BSA. Purified GR1 (peak A, ●) or BSA (peak B, ○) was chromatographed in 50 mM Tris, pH 8, 250 mM NaCl. Peak A corresponds to ≈120 kDa and peak B to ≈70 kDa. a.u., arbitrary units. (*C*) Kinetic mechanism of GR1. Hanes plot for kinetic analysis of GR1 regarding the substrate GSSG is shown; experimental data are represented by symbols and the global fit of all data by a line (R^2 = 0.92). The enzyme assay was performed with 200 μM NADPH and 15–1,000 μM GSSG. Mean values ± SD are shown (n = 3). (*D*) GR assay using GRX1-roGFP2 as a sensor for the actual E_{GSH} generated from the mixture of substrate (GSSG) and product (GSH). Fully oxidized GRX1-roGFP2 was mixed with NADPH (100 μM) and with (○) or without (▽) 0.1 μM *At*GR1 at pH 7.0. 2 min after start of the measurement freshly prepared GSH solution was added to a final concentration of 2 mM. For control, full reduction of the probe was achieved with 10 mM DTT (▼), and full oxidation with 10 mM H_2O_2 (●).

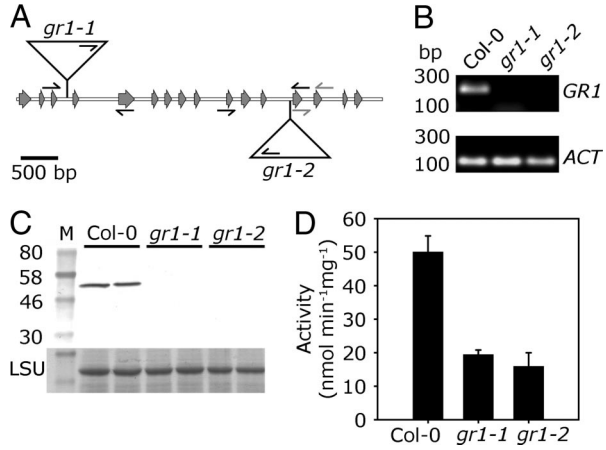

Fig. 2. Isolation and characterization of *gr1* deletion mutants. (*A*) Physical map of the GR1 gene (At3g24170) and T-DNA insertion sites for alleles *gr1-1* and *gr1-2*. Gray arrows indicate exons. Triangles represent the inserted T-DNAs, small black arrows indicate primers used for genotyping and gray arrows primers used for RT-PCR. (*B*) Saturated RT-PCR with primers specific for GR1 cDNA. PCR was performed using cDNA from Col-0, *gr1-1*, and *gr1-2*, respectively, as template. As reference, primers specific for actin 7 were used. (*C*) Protein gel blot analysis with antiserum raised against GR1; 15 μg of total protein of Col-0, *gr1-1*, and *gr1-2* were separated on a 10% SDS/PAGE and electro blotted to nitrocellulose in duplicates. M, prestained molecular mass standard. Equal loading in all lanes is confirmed by staining of the large subunit (LSU) of 1,5-bisphosphate carboxylase/oxygenase (Rubisco). (*D*) GR activity of total leaf protein. Means ± SD (n = 3).

We previously showed that the cytosolic E_{GSH} is ≈−320 mV under nonstress conditions (2), indicating a very high reduction capacity for GSSG. Therefore, we focused on the homeostatic function of GR1, and assessed it at phenotypic, genetic, and biochemical level. The impact of GR1 on cytosolic redox homeostasis was investigated with state-of-the-art redox-sensitive (ro)GFP tools that allow dynamic measurements of E_{GSH} in vivo (3). The results demonstrate TRXh3 in conjunction with NTRA as a GR-independent mechanism of GSSG reduction capable of partially complementing *gr1* mutants. The fundamental function of the NTR/TRX system for GSSG reduction is emphasized by pollen lethality when both reduction systems are lost.

Results

Expression, Purification, and Characterization of *Arabidopsis* GR1. Based on homology, the gene function of locus At3g24170 has been assigned as a cytosolic GR1. The predicted protein shows 61.4% similarity and 23.1% identity with GRs from *E. coli* and *S. cerevisiae*, respectively (Fig. S1). However, the *Arabidopsis* protein contains motifs not found in other GRs including 11 aa before the active centre and a C-terminal extension of 18 aa. To verify that GR1 is a genuine GR, the cDNA was cloned into an expression vector and purified using an introduced N-terminal His-tag. SDS/PAGE analysis of purified GR1 indicated a monomer of ≈60 kDa, which corresponds to the predicated molecular mass of 57.1 kDa calculated for GR1 including the N-terminal His-tag (Fig. 1*A*). Native GR1 is composed of 499 aa and has a molecular mass of 53.8 kDa. Size exclusion chromatography indicated that purified native GR1 eluted significantly earlier than BSA (66 kDa) as a control, suggesting native GR1 was present as a dimer (Fig. 1*B*). The optimal pH for GR1 activity was found to be in the range of 7.2 to 7.6 (Fig. S2*A*); thus, all subsequent experiments were performed at pH 7.4, unless indicated otherwise. Analysis of the catalyzed reaction revealed Michaelis-Menten kinetics with a K_m for the substrate GSSG of 77 μM and a V_{max} of 63 μmol min^{-1} mg^{-1} (Fig. 1*C*). The K_m for the cosubstrate NADPH was 33 μM (Fig. S2*B*). Whereas animal and bacterial GRs are inhibited by 1,3-bis(2-chloroethyl)-1-nitrosourea (BCNU) (22, 23), significant inhibition of recombinant GR1 was observed only at high BCNU concentration >1 mM (Fig. S2*C*), making this compound not suitable for in vivo application.

To further elucidate the efficiency of GR1 for reduction of GSSG, we used recombinant GRX1-roGFP2 as a highly sensitive sensor for the actual E_{GSH} (2, 3). Addition of 2 mM freshly prepared GSH to oxidized GRX1-roGFP2 did not cause a reduction of the sensor unless GR1 and NADPH were present (Fig. 1*D*). In the presence of GR1, roGFP2 was almost completely reduced within 100 min, which was detected as a decrease in the 390/480-nm excitation ratio (Fig. 1*D*). Based on its midpoint potential of −280 mV (24), roGFP2 approaches full reduction only when the degree of GSH oxidation (OxD_{GSH}) drops <0.001%. Thus, GR1 is capable of reducing virtually all GSSG leaving only nanomolar concentrations of GSSG at steady state.

Isolation and Biochemical Characterization of *gr1* Mutants. To further elucidate the function of GR1, 2 different *gr1* T-DNA insertion alleles were obtained from the Salk collection. The homozygous mutants, designated *gr1-1* and *gr1-2*, contain T-DNA insertions in the 3rd and the 12th intron, respectively (Fig. 2*A*). For both mutants, the sequence of genomic DNA flanking the left T-DNA border was sequenced to verify the insertion site (Fig. 2*A*). self-fertilization of heterozygous *gr1* plants resulted in ≈25%

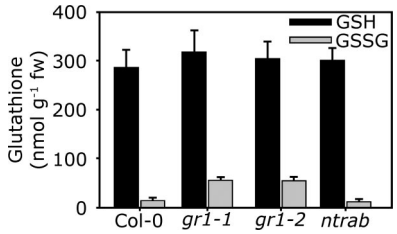

Fig. 3. Glutathione content of *gr1* and *ntra ntrb* deletion mutants. Reduced GSH and GSSG was measured after extraction of 6-week old rosette leaves and derivatisation of thiols with monobromobimane. Means ± SD (n = 8).

homozygous mutants for both alleles (Table S1). Semiquantitative RT-PCR with primers binding to the 13th and the 14th exon (Fig. 2*A*) revealed that both deletion mutants were completely devoid of GR1 mRNA (Fig. 2*B*). Protein gel blot analysis with antiserum against GR1 showed the absence of GR1 protein in both mutant lines (Fig. 2*C*). In total protein extracts from both mutant lines GR activity was reduced by 65% (Fig. 2*D*). The residual GR activity of <20 nmol min^{-1} mg^{-1} is most likely due to the organellar isoform GR2, which is not affected in its abundance in the *gr1* mutant (Fig. S3). To a lower extend, this residual activity can also be attributed to the activity of the NTS system (see below). Loss of GR1 did not affect the amount of GSH. However, the whole cell amount of GSSG determined by HPLC increased ≈4-fold from 13 ± 2 nmol g^{-1} FW in wild-type leaves to 54 ± 7 nmol g^{-1} FW in *gr1* mutants (Fig. 3). Thus, both *gr1* mutants are complete knockouts of GR1.

The *gr1* Plants Have Decreased Buffer Capacity Against ROS. To further elucidate whether the increased GSSG affects E_{GSH}, we expressed GRX1-roGFP2 (3) in the cytosol of *gr1-1* mutants and wild-type plants. Under nonstress conditions, the fluorescence ratio was markedly higher in *gr1* plants (1.5 compared with 0.5 in wild-type plants) (Fig. 4 *A* and *D*). Calibration against 100 mM H_2O_2 to fully oxidize (Fig. 4 *B* and *E*) and 10 mM DTT to fully reduce the sensor (Fig. 4 *C* and *F*) led to similar fluorescence ratio values in both mutant and wild-type. These calibration values and an assumed cytosolic pH of 7.4 gave a value of E_{GSH} = −270 ± 9 mV in *gr1* and ≈−315 ± 9 mV in wild-type leaves. The less negative E_{GSH} in the cytosol of *gr1* plants indicated an increased GSSG concentration in the cytosol, which is in agreement with the HPLC data (Fig. 3). E_{GSH} in plastids and mitochondria was not affected in *gr1* mutants (Fig. S4), indicating that the prime physiological effect of *gr1* deletion was confined to the cytosol.

To test the cytosolic buffer capacity and the ability to counteract an induced oxidation, seedlings were perfused with oxidizing and reducing solutions (Fig. 4*G*). In wild-type plants, GRX1-roGFP2 showed a very small increase in the 405/488-nm ratio from 0.5 to ≈1 after treatment with 1 mM H_2O_2. In contrast, the same treatment of *gr1* seedlings resulted in an increase of the fluorescence ratio from ≈1.4 to ≈4, corresponding to the ratio for fully oxidized GRX1-roGFP2. In contrast, in wild-type seedlings GRX1-roGFP2 was not yet fully oxidized after treatment with 5 mM H_2O_2, showing that the capacity for maintaining GSH in reduced form after H_2O_2 treatment is clearly limited in *gr1* plants. Also, in *gr1* mutants, the GSSG was only reduced very slowly after washout of H_2O_2 (Fig. 4*G*; 13–19.5 min).

Attenuated Cytosolic GSSG Reduction Does Not Confer a Strong Phenotype. The absence of functional GR1 did not result in any obvious phenotype under physiological conditions (Fig. S5). This lack of phenotype is surprising in regard to the high GSSG level measured in the *gr1* mutant, and suggests that accumulation of GSSG is not toxic for the plant or that GSSG is exported from

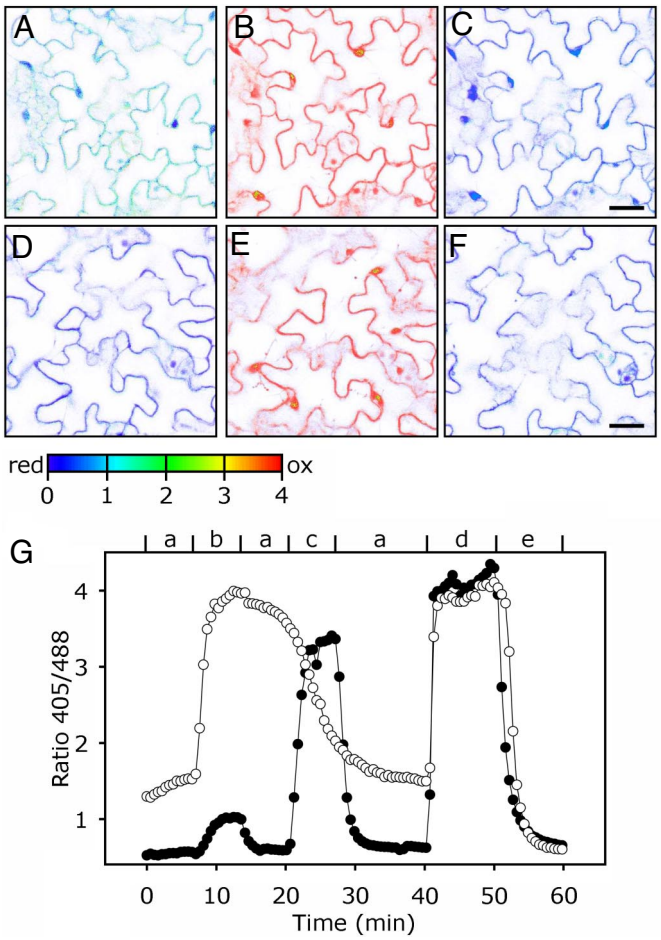

Fig. 4. Oxidation and reduction of glutathione in the cytosol of Col-0 and *gr1-1* plants. Images of wild-type and mutant leaves expressing GRX1-roGFP2 in the cytosol were taken by CLSM with excitation at 405 and 488 nm, respectively. Single images were used for the calculation of the ratio images. (*A–F*) Steady state ratio images of *gr1* (*A–C*) and Col-0 (*D–F*). (*A*) The *gr1* leaf, control, (*B*) *gr1* oxidized with 100 mM H_2O_2, (*C*) *gr1* treated with 10 mM DTT, (*D*) Col-0, untreated control, (*E*) Col-0 oxidized with 100 mM H_2O_2, and (*F*) Col-0 reduced with 10 mM DTT. (Scale bars, 10 μm.) (*G*) Typical time course showing the dynamic response of the cytosolic E_{GSH} in Col-0 (●) and *gr1* (○) to transient oxidation induced by H_2O_2. Small letters indicate perfusion steps: a, ½ MS medium; b, 1 mM H_2O_2; c, 5 mM H_2O_2; d, 100 mM H_2O_2; e, 10 mM DTT. Because treatment of *gr1* leaves with 1 mM H_2O_2 already led to full oxidation of the probe, perfusion step c in this case was done with ½ MS instead of 5 mM H_2O_2.

the cytosol. Also, the *gr1* mutant is not hypersensitive to severe stress conditions like exposure to oxidative stress generating agents (Cu^{2+} ions, H_2O_2) or the heavy metal Cd^{2+} that inactivates metalloproteins and is detoxified by the GSH polymers phytochelatins (Fig. S6). The low level of reduction in absence of a distinct phenotype suggests an alternative cytosolic system for reduction of GSSG.

The Cytosolic TRX System Can Reduce GSSG In Vitro. Therefore, we examined whether the cytosolic NADPH-dependent TRX system can reduce GSSG in vitro. For this purpose, recombinant NTRA and TRXh3 were expressed in *E. coli* and purified. Based on the same amount of protein, the rate of GSSG reduction by NTRA/TRXh3 was ≈200-fold lower than by GR1. In the absence of TRXh3, NTRA on its own did not significantly reduce GSSG (Fig. 5).

Triple Knockouts Are Pollen Lethal. The *ntra ntrb* double mutant had wild-type GSH levels and GSH/GSSG ratios (Fig. 3), but showed

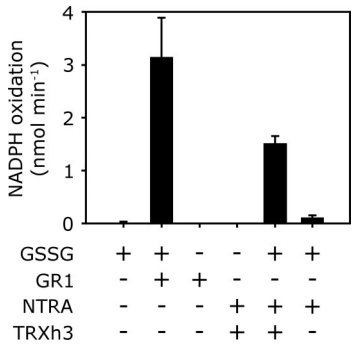

Fig. 5. Biochemical activity of GSSG reduction by NTRA and TRXh3. TRXh3 is first reduced for 30 min with NTRA and NADPH. Activity is monitored as NADPH oxidation. Note that the amount of disulfide reductase protein varied between the assays. Enzymes and substrates were used at the following concentrations: NADPH, 200 μM; GSSG, 400 μM; GR1, 0.01 μM; NTRA, 1 μM; TRXh3, 10 μM. Means ± SD (n = 3).

smaller rosettes (Fig. S5). To test for functional redundancy, we examined whether the TRX system is substituting the lack of GR1 in the *gr1* mutants, we generated triple mutants lacking NTRA, NTRB, and GR1. Both mutant lines, *gr1-1* and *gr1-2*, were crossed with an *ntra ntrb* double knockout. From the F2 generation, mutants homozygous for *ntra* and *ntrb*, but heterozygous for *gr1* were selected and selfed. These mutants segregated a ratio of 1 (*GR1*/*gr1*):1 (*gr1*/*gr1*) with no homozygous triple mutant for either *gr1* allele (Table S2), suggesting that triple mutants are lethal. Lack of aborted seeds (Fig. S7) indicated a pollen lethal effect while female transmission of *gr1* was not impaired.

To further test whether the triple mutation affects male fertility, pollen of a *GR1*/*gr1-1 ntra ntrb* was transferred to wild-type stigma. Progeny testing failed to identify plants heterozygous for *gr1-1* (Table 1), suggesting that no *gr1-1 ntra ntrb* pollen had successfully fertilized the wild-type ovules. Alexander staining (25) revealed no cytoplasmic or pollen wall abnormalities. The reciprocal cross did result in 50% *GR1*/*gr1* plants, which again confirmed that female transmission of the defective *gr1* allele in the *ntra ntrb* background was normal.

The genetic evidence suggests that at least one of the cytosolic disulfide Rs, GR1, NTRA, or NTRB, is required for development of the male gametophyte. To test this hypothesis, the presence of the 3 transcripts was measured in mature pollen. Semiquantitative RT-PCR indicated that GR1 and NTRA were both expressed in pollen, whereas no signal could be detected for NTRB Fig. S8. In flowers, GR1 and both NTR isoforms were detected. Selfing of a mutant homozygous for *ntra* and heterozygous for *gr1* resulted in a 1:1 segregation of the progeny (15:15, $\chi^2 = 0$, $P = 1$) expected if the double knockout is lethal. In combination with the *ntrb* knockout, *gr1* segregated with a 1:2:1 ratio (7:17:6; $\chi^2 = 0.6$, $P > 0.5$).

Table 1. Reciprocal cross between *GR1/gr1-1 ntra/ntra ntrb/ntrb* and Col-0

A:	Female parent	×	Male parent	Progeny genotype	
	GR1/gr1-1 ntra/ntra ntrb/ntrb	×	Col-0	*GR1/gr1-1 NTRA/ntra NTRB/ntrb*	*GR1/GR1 NTRA/ntra NTRB/ntrb*
	Frequency*			13	16
B:	Female parent	X	Male parent	Progeny genotype	
	Col-0	×	*GR1/gr1-1 ntra/ntra ntrb/ntrb*	*GR1/gr1-1 NTRA/ntra NTRB/ntrb*	*GR1/GR1 NTRA/ntra NTRB/ntrb*
	Frequency			0	38

*Twenty-nine progeny were genotyped by PCR. $\chi^2 = 0.416$ for 1:1 segregation, $P = 0.52$.

†Thirty-eight progeny were genotyped by PCR. $\chi^2 = 29$ for 1:1 segregation, $P = 0$.

Discussion

Catalytic Activity of *Arabidopsis* GR1. *Arabidopsis* GR1 is present as a FAD-bound homodimer (Fig. 1) similar to homologous flavoprotein disulfide reductases from other organisms (15). The K_m value of 77 μM for the substrate GSSG is similar to K_m values reported for GRs from *E. coli* (61 μM), yeast (55 μM), and human (72 μM) (26–28). GRX1-roGFP2 reports the actual E_{GSH} (3), and due to its midpoint potential of −280 mV (24), allows the determination of residual amounts of GSSG in the presence of GR and the second substrate NADPH. Both, in vitro (Fig. 2) and in vivo (Fig. 4) GR1 maintain an E_{GSH} of ≈−310 mV, which is consistent with earlier in vivo measurements in *Arabidopsis* and HeLa cells (2, 3). Due to irreversibility of the reaction, GR1 can, thus, maintain nanomolar GSSG concentrations in the cytosol.

GR1 Is Not Essential for Plant Development. In mammals and bacteria, the inhibitor BCNU has been used (22, 23). However, it does not inhibit plant GR1. Thus, to confirm the importance of GR1, T-DNA knockout mutants were selected and characterized. In the absence of detectable GR1 transcript and GR1 protein in both isolated mutants and no elevation of organellar GR2 protein, the remaining GR activity of total protein extract of ≈35% in *gr1* mutants compared with wild-type plants can be attributed to GR2 activity (29) and possibly other cytosolic reduction systems. The 65% share of the overall GR activity in leaf extracts for cytosolic GR1 is much higher than 20% activity associated with the cytosol in pea leaves (30).

ATP-binding cassette (ABC) transporters with micromolar K_m values have been proposed as backup systems for insufficient cytosolic GR activity (31). Although roGFP at this stage is not capable of detecting increased accumulation of GSSG in the ER or the vacuole, the absence of continuous accumulation of GSSG and the less reducing cytosolic E_{GSH} of *gr1* mutants rather suggest an alternative cytosolic reduction system with lower efficiency than GR1.

TRX and NTR Can Replace GR In Vitro. An E_{GSH} of −270 mV in the cytosol is still sufficiently negative to maintain metabolic functions under normal conditions, which is consistent with reports of GR deletion mutants in *S. cerevisiae* (32). The use of a ratiometric probe in this work allowed dynamic in vivo measurements of E_{GSH} under induced oxidative stress. These measurements, showed (*i*) that the buffer capacity of *gr1* against ROS is significantly diminished, and (*ii*) that another less efficient reduction system is in place (Fig. 4*G*). In mammalian cells, GR and NTR share many common features, including similar primary and tertiary structures and high similarities of active site residues (33). However, lack of electrostatic attraction in the potential GSSG binding pocket prevents efficient GSSG reduction by human NTR (34). However, this observation cannot be directly transferred to plants, because GR1 and NTRA in this case are not related to each other (35). Also, our results for *Arabidopsis* clearly disproved the hypothesis of direct GSSG reduction for NTRA (Fig. 5). Only together with TRX and NADPH as electron donor, NTRA is capable of reducing GSSG, suggesting that the TRX system as a whole may constitute a backup system for GR1. When measured in vitro, the activity of NTRA/TRXh3 toward GSSG was 200-fold lower than the activity of GR1 (Fig. 5). This large difference in activity high-

lights the difficulties of direct extrapolation from in vitro data to the in vivo situation where the *gr1* mutant still has a considerable reduction capacity for GSSG (Fig. 4). Within the pool of 11 cytosolic type h TRX (36), some isoforms may be more efficient than the tested TRXh3. Also, the in vitro assay does not consider the relative abundance of the respective oxidoreductases. The abundance of documented ESTs indicates that NTR (60 ESTs) and TRXh (>100 ESTs) may be far more abundant than GR1 (30 ESTs), at least at mRNA level. The situation in the *Arabidopsis gr1* mutant to some extent resembles the naturally occurring situation in *Drosophila melanogaster*, where the TRX system substitutes for the lacking GR (9). It can also not be excluded that some other alternative GSSG reduction systems may act in *Arabidopsis* and contribute to maintenance of GSH redox homeostasis in *gr1* mutants. A multifunctional TRX GR has been found in *Schistosoma mansoni*, which has an N-terminal GRX-like domain for TRX-independent GSSG reduction (37). In *Synechocystis*, which also lacks a genuine GR, NTR-reducible GRXs may act as intermediate reducers of GSSG (38). Due to the high number of isoforms, further dissection of individual contributions to GSSG is a difficult challenge. However, the genetic evidence provided here (see below) clearly shows the need of either GR1 or NTR in plants. The NTRs are highly similar across the plant kingdom, and wheat NTR is a highly efficient reducer of *Arabidopsis* TRXh. Thus, it can be assumed that the backup of cytosolic GR1 by the NTR/TRX system is universal across plant species. In contrast to *S. cerevisiae*, where mutual functional backup between NTR/TRX and GR has been shown (20), redundancy between GR and the NTR/TRX system in plants seems to be restricted to the cytosol, because mutants lacking organellar GR2 are embryo lethal (12). Deletion of GR1 may be tolerable, because oxidative stress in the cytosol is relatively low compared with plastids and mitochondria (39). A drop in cytosolic E_{GSH} is likely to gradually affect downstream signaling and developmental processes. Antisense lines for *Arabidopsis* GSH1 indicated that 5% of wild-type GSH, which would result in an E_{GSH} of ≈ -240 mV, already limits the growth rate and renders plants more sensitive to environmental stress (40). Progressive growth inhibition and increasing stress sensitivity is also apparent for the even more severely affected *rml1* mutant, which has <5% of wild-type GSH, and embryo lethal *gsh1* deletion mutants (41, 42). Deletion of GR and a concomitant 21-fold increase in GSSG have been reported to cause oxidation of GRXs in *S. cerevisiae* (20). Even though this oxidation does not have an immediate effect on plant development, it can be assumed that excessive oxidation of GRXs can affect downstream processes under conditions of severe stress.

Either GR1 or NTRA Is Required for Pollen Viability. Genetic evidence for the functional overlap between GR1 and the TRX system was gained from the combination of the *gr1* mutation with a *ntra ntrb* double knockout. In *Arabidopsis*, the *ntra* and *ntrb* deletion mutants on their own do not show any phenotype (16). A growth phenotype of the *ntra ntrb* double knockout indicated functional redundancy between the 2 NTRs in the diploid phase (18). Interestingly, our present results also show functional overlap between cytosolic GR1 and NTRA during the haploid phase. Cross-pollination experiments showed that the lethal phenotype can be attributed to the male gametophyte, whereas oocytes with the triple mutation in GR1, NTRA, and NTRB genes are viable, as shown by the segregations after pollination with the wild-type (Table 1, Fig. S7). The difference between male and female gametophytes remains elusive, but it may be that pollen depends on a more robust redox buffer system. Pollen tube growth is associated with increased ROS production (43), which may be deleterious in the triple mutant. Oocytes, in contrast, are resting and also much better protected by maternal tissues. Transmission of defective *gr1* alleles in pollen can only occur in the presence of functional NTRA, suggesting that GR1 and NTRA proteins have a major role in pollen fertility. Indeed, detection of GR1 and NTRA transcripts in pollen are also supported by proteomic analysis (44). However, NTRB mRNAs were hardly detected in pollen, and this protein has never been found in the pollen proteome. The fact that no NTRB transcript was found in pollen and that *gr1* in a homozygous *ntrb* background segregated 1:2:1 unambiguously shows that NTRB is not important for *gr1* transmission. However, this does not exclude the possibility that NTRB might contribute to cytosolic GSH redox homeostasis in mature plants, especially under conditions of severe oxidative stress. Because *gr1 ntra* pollen are not viable, homozygous mutants required to test for the function of GR1 and NTRs in embryonic tissue and mature plants can only be generated from conditional knockouts activated after fertilization. RNAi and inducible expression constructs will be helpful to investigate this question in more detail.

In summary, our study shows that NTRA together with TRXh3 exhibit functional redundancy with cytosolic GR1. Biochemical and genetic evidence shows that GR1 constitutes the main GR activity in *Arabidopsis*. Despite the presence of an efficient backup system, deletion of GR1 significantly lowers the buffering capacity of the cytosolic GSH pool against ROS. The delayed reduction of GSSG after an exogenously triggered oxidation in the *gr1* mutant indicates that *gr* mutants expressing GRX1-roGFP2 may constitute a suitable system for detection of stress-induced ROS signals.

Materials and Methods

Plant Material and Growth Conditions and Treatments. Plants were soil grown in 8.5:15.5-h day/light cycle at a temperature between 18 and 22 °C, 100 μE m^{-2} s^{-1} and 50% humidity. For Confocal laser scanning fluorescence microscopy (CLSM) analysis, transgenic seeds were surface sterilized and grown on 0.5× Murashige and Skoog (MS) medium (pH 5.7, 1% sucrose, 0.7% agar). Rosette leaves of 19- to 22-d old T_2-seedlings were used for imaging.

For stress treatments of in vitro seedlings, seeds were surface sterilized and plated on 0.5× MS medium including Gamborg B5 vitamins [pH 5.7, 1% (wt/vol) sucrose, 0.8% (wt/vol) plant agar] (Duchefa). To supplement the growth medium with H_2O_2, $CdCl_2$, and $CuSO_4$ at various concentrations, appropriate amounts of the respective filter-sterilized stock solutions were added to 0.5× MS medium before gelling.

Isolation of Total RNA and Semiquantitative RT-PCR. Total RNA was extracted from *Arabidopsis* leaves, pollen, or inflorescences, and reverse transcribed in cDNA; cDNA was subsequently used for semiquantitative RT-PCR. For details, see *SI Materials and Methods*.

Molecular Cloning and Plasmid Constructs. Cloning and expression of proteins is described in *SI Materials and Methods*.

Protein Purification. Recombinant roGFP protein was cloned, expressed, and purified as previously described (2). For all other proteins, details are described in *SI Materials and Methods*.

Identification of T-DNA Insertion Lines. Two T-DNA insertion lines, *gr1-1* and *gr1-2*, were obtained form the SALK collection, and characterized as described in *SI Materials and Methods*. Alleles of *ntra* and *ntrb* were identified as described (18).

Mutant Crosses and Pollen Competition. For generation of *ntra ntrb gr1* triple mutant, the *ntra ntrb* double mutant was crossed with either *gr1-1* or *gr1-2*. The F_1 plants were selfed, and plants with the desired genotype were selected in the F_2 generation. Pollen competition experiments were performed as described (18).

Protein Extraction from *Arabidopsis* Leaves. Protein was extracted from 250-mg ground leaf material using extraction buffer (50 mM Hepes, pH 7.4/10 mM KCl/1 mM EDTA/1 mM EGTA/10% vol/vol glycerol) supplemented with 1 mM PMSF. The extract were desalted with NAP5 columns (GE Healthcare), and resuspended in 1 mM K_2HPO_4/KH_2PO_4, pH 7.4/1 mM EDTA. Protein concentrations were determined by Bradford.

GR Activity. Twenty micrograms of proteins were assayed in 100 mM K_2HPO_4/KH_2PO_4, pH 7.4/1 mM EDTA/750 μM DTNB/200 μM NADPH/400 μM GSSG. Absorbance was measured at 412 nm. NADPH and GSSG were always freshly prepared. For inhibition experiments, BCNU was dissolved in ethanol and added to the concentrations indicated.

Antibody Production and Protein Gel Blot Analysis. Experimental details are provided in *SI Materials and Methods*.

HPLC Analysis of Glutathione. GSH and GSSG were analyzed from 7-week-old, soil grown *Arabidopsis* plants as described (2). The amount of GSH measured after extraction with NEM refers to the amount of GSSG present in the sample. After subtraction form the total GSH pool measured after extraction with DTT, the difference corresponds to the amount of GSH present in the sample.

Redox-Sensitive GFP Imaging and GR Assay Using GRX1-roGFP. Ratiometric imaging of roGFP, perfusion experiments, and image analysis were done as described previously (45).

ACKNOWLEDGMENTS. This work was supported by Centre National de la Recherche Scientifique Genoplante Project GNP0508, the Agence Nationale de la Recherche (ANR), ANR-Blanc Grant 06-0047 (to W.S.), and in part by grants to R.H.

1. Mittler R, Vanderauwera S, Gollery M, Van Breusegem F (2004) Reactive oxygen gene network of plants. *Trends Plants Sci* 9:490–498.
2. Meyer AJ, et al. (2007) Redox-sensitive GFP in *Arabidopsis thaliana* is a quantitative biosensor for the redox potential of the cellular glutathione redox buffer. *Plant J* 52:973–986.
3. Gutscher M, et al. (2008) Real-time imaging of the intracellular glutathione redox potential. *Nat Methods* 5:553–559.
4. Noctor G, Foyer CH (1998) Ascorbate and glutathione: Keeping active oxygen under control. *Annu Rev Plant Physiol Plant Mol Biol* 49:249–279.
5. Ball L, et al. (2004) Evidence for a direct link between glutathione biosynthesis and stress defense gene expression in Arabidopsis. *Plant Cell* 16:2448–2462.
6. Meyer AJ (2008) The integration of glutathione homeostasis and redox signaling. *J Plant Physiol* 165:1390–1403.
7. Xing S, Rosso MG, Zachgo S (2005) ROXY1, a member of the plant glutaredoxin family, is required for petal development in *Arabidopsis thaliana. Development* 132:1555–1565.
8. Ndamukong I, et al. (2007) SA-inducible Arabidopsis glutaredoxin interacts with TGA factors and suppresses JA-responsive PDF1.2 transcription. *Plant J* 50:128–139.
9. Kanzok SM, et al. (2001) Substitution of the thioredoxin system for glutathione reductase in *Drosophila melanogaster. Science* 291:643–646.
10. Krauth-Siegel RL, Comini MA (2008) Redox control in trypanosomatids, parasitic protozoa with trypanothione-based thiol metabolism. *BBA-Gen Subjects* 1780:1236–1248.
11. Chew O, Whelan J, Millar AH (2003) Molecular definition of the ascorbate-glutathione cycle in Arabidopsis mitochondria reveals dual targeting of antioxidant defenses in plants. *J Biol Chem* 278:46869–46877.
12. Tzafrir I, et al. (2004) Identification of genes required for embryo development in Arabidopsis. *Plant Physiol* 135:1206–1220.
13. Zimmermann P, Hirsch-Hoffmann M, Hennig L, Gruissem W (2004) GENEVESTIGATOR. Arabidopsis microarray database and analysis toolbox. *Plant Physiol* 136:2621–2632.
14. Bouché N, Bouchez D (2001) Arabidopsis gene knockout: Phenotypes wanted. *Curr Opin Plant Biol* 4:111–117.
15. Argyrou A, Blanchard JS (2004) Flavoprotein disulfide reductases: Advances in chemistry and function. *Progress in Nucleic Acid Research and Molecular Biology*, ed Moldave K (Elsevier Academic, San Diego), Vol 78, pp 89–142.
16. Reichheld JP, Meyer E, Khafif M, Bonnard G, Meyer Y (2005) AtNTRB is the major mitochondrial thioredoxin reductase in *Arabidopsis thaliana. FEBS Lett* 579:337–342.
17. Laloi C, et al. (2001) Identification and characterization of a mitochondrial thioredoxin system in plants. *Proc Natl Acad Sci USA* 98:14144–14149.
18. Reichheld J-P, et al. (2007) Inactivation of thioredoxin reductases reveals a complex interplay between thioredoxin and glutathione pathways in Arabidopsis development. *Plant Cell* 19:1851–1865.
19. Carmel-Harel O, Storz G (2000) Roles of the glutathione- and thioredoxin-dependent reduction systems in the *Escherichia coli* and *Saccharomyces cerevisiae* response to oxidative stress. *Annu Rev Microbiol* 54:439–461.
20. Trotter EW, Grant CM (2003) Non-reciprocal regulation of the redox state of the glutathione-glutaredoxin and thioredoxin systems. *EMBO Rep* 4:184–188.
21. Song J-Y, Cha J, Lee J, Roe J-H (2006) Glutathione reductase and a mitochondrial thioredoxin play overlapping roles in maintaining iron-sulfur enzymes in fission yeast. *Eukaryot Cell* 5:1857–1865.
22. Schafer FQ, Buettner GR (2001) Redox environment of the cell as viewed through the redox state of the glutathione disulfide/glutathione couple. *Free Radic Biol Med* 30:1191–1212.
23. Starke PE, Farber JL (1985) Endogenous defenses against the cytotoxicity of hydrogen peroxide in cultured rat hepatocytes. *J Biol Chem* 260:86–92.
24. Dooley CT, et al. (2004) Imaging dynamic redox changes in mammalian cells with green fluorescent protein indicators. *J Biol Chem* 279:22284–22293.
25. Alexander M (1969) Differential staining of aborted and nonaborted pollen. *Stain Technol* 44:117–122.
26. Savvides SN, Karplus PA (1996) Kinetics and crystallographic analysis of human glutathione reductase in complex with a xanthene inhibitor. *J Biol Chem* 271:8101–8107.
27. Henderson G, et al. (1991) Engineering the substrate specificity of glutathione reductase toward that of trypanothione reduction. *Proc Natl Acad Sci USA* 88:8769–8773.
28. Massey V, Williams CH, Jr (1965) On the reaction mechanism of yeast glutathione reductase. *J Biol Chem* 240:4470–4480.
29. Chew O, Rudhe C, Glaser E, Whelan J (2003) Characterization of the targeting signal of dual-targeted pea glutathione reductase. *Plant Mol Biol* 53:341–356.
30. Edwards EA, Rawsthorne S, Mullineaux P (1990) Subcellular distribution of multiple forms of glutathione reductase in leaves of pea (*Pisum sativum* L.). *Planta* 180:278–284.
31. Foyer CH, Theodoulou FL, Delrot S (2001) The functions of inter- and intracellular glutathione transport systems in plants. *Trends Plants Sci* 6:486–492.
32. López-Mirabal HR, Winther JR (2008) Redox characteristics of the eukaryotic cytosol. *BBA-Mol Cell Res* 1783:629–640.
33. Sandalova T, Zhong L, Lindqvist Y, Holmgren A, Schneider G (2001) Three-dimensional structure of a mammalian thioredoxin reductase: Implications for mechanism and evolution of a selenocysteine-dependent enzyme. *Proc Natl Acad Sci USA* 98:9533–9538.
34. Urig S, Lieske J, Fritz-Wolf K, Irmler A, Becker K (2006) Truncated mutants of human thioredoxin reductase 1 do not exhibit glutathione reductase activity. *FEBS Lett* 580:3595–3600.
35. Meyer Y, et al. (2006) Evolution of redoxin genes in the green lineage. *Photosynth Res* 89:179–192.
36. Meyer Y, et al. (2008) Glutaredoxins and thioredoxins in plants. *BBA-Mol Cell Res* 1783:589–600.
37. Alger HM, Williams DL (2002) The disulfide redox system of *Schistosoma mansoni* and the importance of a multifunctional enzyme, thioredoxin glutathione reductase. *Mol Biochem Parasitol* 121:129–139.
38. Marteyn B, Domain F, Legrain P, Chauvat F, Cassier-Chauvat C (2009) The thioredoxin reductase-glutaredoxins-ferredoxin crossroad pathway for selenate tolerance in *Synechocystis* PCC6803. *Mol Microbiol* 71:520–532.
39. Foyer CH, Noctor G (2003) Redox sensing and signalling associated with reactive oxygen in chloroplasts, peroxisomes and mitochondria. *Physiol Plant* 119:355–364.
40. Xiang C, Werner BL, Christensen EM, Oliver DJ (2001) The biological functions of glutathione revisited in Arabidopsis transgenic plants with altered glutathione levels. *Plant Physiol* 126:564–574.
41. Vernoux T, et al. (2000) The ROOT MERISTEMLESS1/CADMIUM SENSITIVE2 gene defines a glutathione-dependent pathway involved in initiation and maintenance of cell division during postembryonic root development. *Plant Cell* 12:97–110.
42. Cairns NG, Pasternak M, Wachter A, Cobbett CS, Meyer AJ (2006) Maturation of Arabidopsis seeds is dependent on glutathione biosynthesis within the embryo. *Plant Physiol* 141:446–455.
43. Cardenas L, McKenna ST, Kunkel JG, Hepler PK (2006) NAD(P)H Oscillates in Pollen Tubes and Is Correlated with Tip Growth. *Plant Physiol* 142:1460–1468.
44. Noir S, Brautigam A, Colby T, Schmidt J, Panstruga R (2005) A reference map of the *Arabidopsis thaliana* mature pollen proteome. *Biochem Biophys Res Commun* 337:1257–1266.
45. Schwarzländer M, et al. (2008) Confocal imaging of glutathione redox potential in living plant cells. *J Microsc* 231:299–316.

Table S1. Segregation analysis of *gr1-1* (A) and *gr1-2* (B)

A:	Parent plant genotype		Progeny genotype		
	GR1/*gr1-1*	→	*GR1*/*GR1*	*GR1*/*gr1-1*	*gr1-1*/*gr1-1*
	Frequency		**11**	**18**	**11**
40 progeny were genotyped by PCR. χ^2 for 1:2:1 segregation: 0.4; P>0.5					

B:	Parent plant genotype		Progeny genotype		
	GR1/*gr1-2*	→	*GR1*/*GR1*	*GR1*/*gr1-2*	*gr1-2*/*gr1-2*
	Frequency		**8**	**16**	**6**
30 progeny were genotyped by PCR. χ^2 for 1:2:1 segregation: 0.4; P>0.5					

Table S2. Segregation analysis of *gr1-1* (A) and *gr1-2* (B) mutant allele in a homozygous *ntra ntrb* mutant

A:	Parent plant genotype		Progeny genotype		
	GR1/*gr1-1*		*GR1*/*GR1*	*GR1*/*gr1-1*	*gr1-1*/*gr1-1*
	ntra/*ntra*	→	*ntra*/*ntra*	*ntra*/*ntra*	*ntra*/*ntra*
	ntrb/*ntrb*		*ntrb*/*ntrb*	*ntrb*/*ntrb*	*ntrb*/*ntrb*
	Frequency		**22**	**20**	**0**

42 progeny were genotyped by PCR. χ^2 for 1:1 segregation: 0.095; P=0.76

B:	Parent plant genotype		Progeny genotype		
	GR1/*gr1-2*		*GR1*/*GR1*	*GR1*/*gr1-2*	*gr1-2*/*gr1-2*
	ntra/*ntra*	→	*ntra*/*ntra*	*ntra*/*ntra*	*ntra*/*ntra*
	ntrb/*ntrb*		*ntrb*/*ntrb*	*ntrb*/*ntrb*	*ntrb*/*ntrb*
	Frequency		**27**	**30**	**0**

57 progeny were genotyped by PCR. χ^2 for 1:1 segregation: 0.158; P=0.69

Supporting Information

Marty et al. 10.1073/pnas.0900206106

SI Materials and Methods

Semiquantitative RT-PCR. Total RNA was extracted from *Arabidopsis* leaf material ground in liquid N_2. RNA was extracted with TRIzol (Invitrogen). RNA was reverse transcribed in cDNA using the M-MLV Reverse Transciptase kit (Promega). glutathione reductase (GR)1 cDNA was PCR amplified with the primers 5′-CATACCACCACTAGCTGTAGTG-3′ and 5′-TGCATGATCTCAGCTGCATCAG-3′. The reference cDNA of the constitutively expressed actin 7 was amplified with primers 5′-CAACCGGTATTGTGCTCGATTC-3′ and 5′-GAGTGAGTCTGTGAGATCCCG-3′. PCR was performed with Taq polymerase (New England Biolabs) in a standard PCR program.

Isolated spores from male gametophyte were obtained by modification of the protocol of Honys and Twell (1); 500 mg of *Arabidopsis* inflorescences were collected and gently ground using a mortar and pestle in 5 mL of 0.3 M mannitol. The slurry was filtered through 100 and 60 μM nylon mesh. Mixed spores were concentrated by centrifugation (15 mL Falcon tubes, 450 × *g*, 3 min, 4 °C). Concentrated spores were washed in 1 mL of 0.3 M mannitol, and spores were concentrated again by centrifugation (Eppendorf tubes, 2,000 × *g*, 1 min, 4 °C) and stored at −80 °C. The purity of isolated fractions was determined by light microscopy and DAPI staining. Viability was assessed by fluorescein 3′,6′-diacetate (FDA) treatment. RNA isolation and RT-PCR experiments were performed as described above; cDNA were amplified with the following primers: *GR1* forward primer, 5′-CTAATATACCTAGCATATGGGCTGTAGGAG-3′, and reverse primer, 5′-TCATAGATTTGTCTTAGGTTTGGG-3′. *GR2* forward primer, 5′-GGATTTCGTTGGAGAGCAGATGTCTTTAAGA-3′, and reverse primer, 5′-CTACACCCCAGCAGCTGTTTTAG-3′. *NTRA* forward primer, 5′-GCAAAATGTGTTGGATCTCAATGAG-3′, and reverse primer, 5′-CATGGATCCTTCTCCTACAGCTTC-3′. *NTRB* forward primer, 5′-CGAAAGCTTTGCACGGCTTGGTGGTG-3′, and reverse primer, 5′-GATCAATCAACAATAACTCAATGACCT-3′. *SPIK* forward primer, 5′-GTATAGCAGTGAGCCTACAATG-3′, and reverse primer, 5′-TCATTACTCAAAATCGAAAGAG-3′. *EF1α* forward primer, 5′-CTAAGGATGGTCAGACCCG-3′, and reverse primer, 5′-CTTCAGGTATGAAGACACC-3′.

Molecular Cloning and Plasmid Constructs. For expression of recombinant protein, *GR1* was amplified by PCR with Phusion polymerase (Finnzymes) using a cDNA template. The AseI and BamHI restriction sites (underlined in primer sequence) were added to forward (5′-ATTAATGAGAATCTTTATTTTCAGGGCATGGCGAGGAAGATGCTTG-3′) and reverse (5′-GGATCCTCATAGATTTGTCTTAGGTTTGG-3′) primers, respectively. PCR product was purified and blunt ligated into the MluNI site of pCAP (Roche). Accuracy of the construct and the cloned sequence was confirmed by sequencing (Seqlab). Subsequently, the *GR1* sequence was cut out with AseI and BamHI and cloned into pET28a (Novagen) behind an N-terminal His_6 tag.

NTRA was PCR amplified using the primers 5′-GGGGACAAGTTTGTACAAAAAAGCAGGCTCAATGGAAACTCACAAAACCA-3′, and 5′-GGGGACCACTTTGTACAAGAAAGCTGGGTCTCAATCACTCTTACCCTCCT-3′. TRXh3 was amplified by PCR with the primers 5′-GGGGACAAGTTTGTACAAAAAAGCAGGCTCAATGGCCGCAGAAGGAGAAG-3′ and 5′-GGGGACCACTTTGTACAAGAAAGCTGG*GTCTCAAGC*AGCAGCAACAACTG-3′. Both PCR products were cloned into pETG10 (Novagen) to generate an N-terminal His_6 tag using the Gateway technology (Invitrogen).

GRX1-roGFP2 (2) was PCR amplified with Phusion polymerase (Finnzymes) using the primers 5′-GATCCATGGCTCAAGAGTTTGTGA-3′ and 5′-GTCGACTTACTTGTACAGCTCGTCC-3′ to add BamHI and SalI restriction sites. The PCR product was cloned blunt-end into the vector pCAP (Roche). The GRX1-roGFP2 was then subcloned into the expression vector pBinAR with BamHI and SalI. The construct was transformed into the *Agrobacterium* strain AGL-1 and used for *Arabidopsis* transformation.

Protein Purification. Recombinant roGFP protein was cloned, expressed, and purified as previously described (3). For all other proteins the pET constructs were transformed into *Escherichia coli* HMS 174 cells. Cells were grown at 37 °C to an OD_{600} of 0.8 in selective media containing 50 μg/mL kanamycin. Protein expression was induced by adding IPTG to a final concentration of 1 mM and cells were harvested after 4 h. Cells were pelleted by centrifugation and resuspended in 50 mM Tris·HCl, pH 8/250 mM NaCl buffer supplemented with 0.5 mM PMSF. After sonication the cell debris was pelleted by centrifugation and filtered through a 45 μM sterile filter. Soluble proteins were loaded on a Ni^{2+}-NTA column (Amersham) for 30 min with a flow rate of 1 mL min^{-1}. The loaded column was washed with 10 mL wash buffer (50 mM Tris·HCl, pH 8/250 mM NaCl/80 mM imidazole). Last, the protein was eluted with elution buffer (wash buffer with 250 mM imidazole). The protein concentration was determined by Bradford.

Identification of T-DNA Insertion Lines. Both mutant alleles *gr1-1* (SALK_105794) and *gr1-2* (SALK_060425) were obtained form the SALK collection. Homozygous knock-out plants were identified by PCR using gene-specific primers and primers binding to the left border of the T-DNA. The following primers were used for *gr1-1*: GR1-1_f 5′-TCGTCTATGGAGCTACTTACGGTGG-3′ GR1-1_r 5′-CGCAAAAATATCCAATCTACTGAGCAC-3′, *gr1-2:* GR1-2_f 5′-CTCCAGCTGTCTAAGGATGTATC-3′ GR1-2_r 5′-CTACTGCTTCTTCTTCGCTGAGAC-3′ T-DNA left border was 5′-GACCGCTTGCTGCAACTCTCTCAGG-3′. PCR performed with DNA from homozygous knockout plant and gene specific primers yielded no PCR product. T-DNA insertions were confirmed by PCR with the following combinations: GR1-1: GR1-1_r and T-DNA left border primer, GR1-2_f and T-DNA left border primer. Alleles of *ntra* and *ntrb* were identified as described (4).

Antibody Production and Protein Gel Blot Analysis. Antiserum against *At*GR1 and *At*GR2 was generated by injection of purified recombinant protein in rabbit. For protein gel blot analysis, 15 μg of extracted proteins were separated by discontinuous SDS/PAGE in MiniProtean II cells according to Laemmli (Bio-Rad). Proteins were transferred to nitrocellulose using the Mini Trans-Blot system (BioRad). To confirm a successful transfer and equal loading, the nitrocellulose membrane was stained with Ponceau [0.1% Ponceau S (wt/vol) in 5% acetic acid]. Subsequently, the membrane was blocked over night at room temperature with 5% Milk powder in TBS (20 mM Tris/137 mM NaCl, pH 7.6) supplemented with 0.1% (vol/vol) Tween 20. The membrane was washed 3 times with 0.5% Milk powder in TBS and 0.01% Tween and incubated with primary antiserum at

dilution of 1:5,000 for 2 h. After washing 3 times for 5 min with 0.5% Milk powder in TBS, the membrane was incubated with secondary antibody [Anti-rabbit IgG-Alkaline Phosphatase (AP) Conjugate, 1:10,000] for 1 h and washed twice with AP buffer (100 mM Tris·HCl, pH 9.5/100 mM NaCl/50 mM $MgCl_2$). The AP reaction was done by adding the substrate nitroblue tetrazolium/5-bromo-5-chloro-3-indolyl phosphate (Roche).

1. Honys D, Twell D (2004) Transcriptome analysis of haploid male gametophyte development in Arabidopsis. *Genome Biol* 5:R85.
2. Gutscher M, et al. (2008) Real-time imaging of the intracellular glutathione redox potential. *Nat Methods* 5:553–559.
3. Meyer AJ, et al. (2007) Redox-sensitive GFP in *Arabidopsis thaliana* is a quantitative biosensor for the redox potential of the cellular glutathione redox buffer. *Plant J* 52:973–986.
4. Reichheld J-P, et al. (2007) Inactivation of thioredoxin reductases reveals a complex interplay between thioredoxin and glutathione pathways in Arabidopsis development. *Plant Cell* 19:1851–1865.

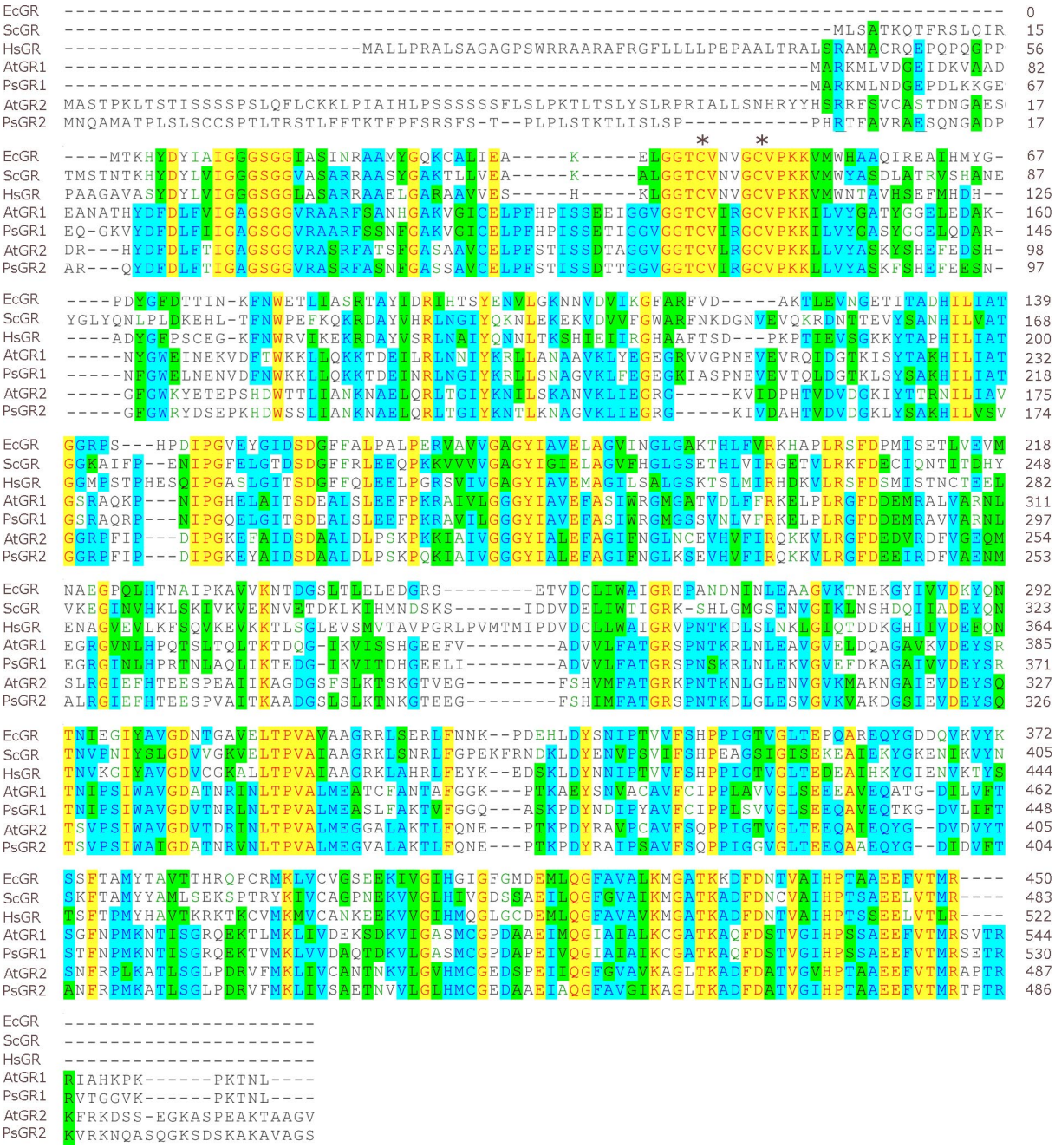

Fig. S1. Protein alignment of *Arabidopsis* GRs with 5 homologues from other species. Identical residues are highlighted in yellow, conservative residues are highlighted in cyan, and blocks of similar residues in green. Green letters on white background represent residues with weak similarity. *Ec*GR: *Escherichia coli* (gi|121674); *Sc*GR: *Saccharomyces cerevisiae* (gi|1708060); *Hs*GR: *Homo sapiens* (gi|14916998); *At*GR2: *Arabidopsis thaliana* (At3g54660; gi|1170040); *Ps*GR2: *Pisum sativum* (gi|121676). *At*GR1: *A. thaliana* (At3g24170; gi|1346194); *Ps*GR1: *P. sativum* (gi|2500116). Cysteines within the redox active center are marked (*). The alignment was performed with ClustalX.

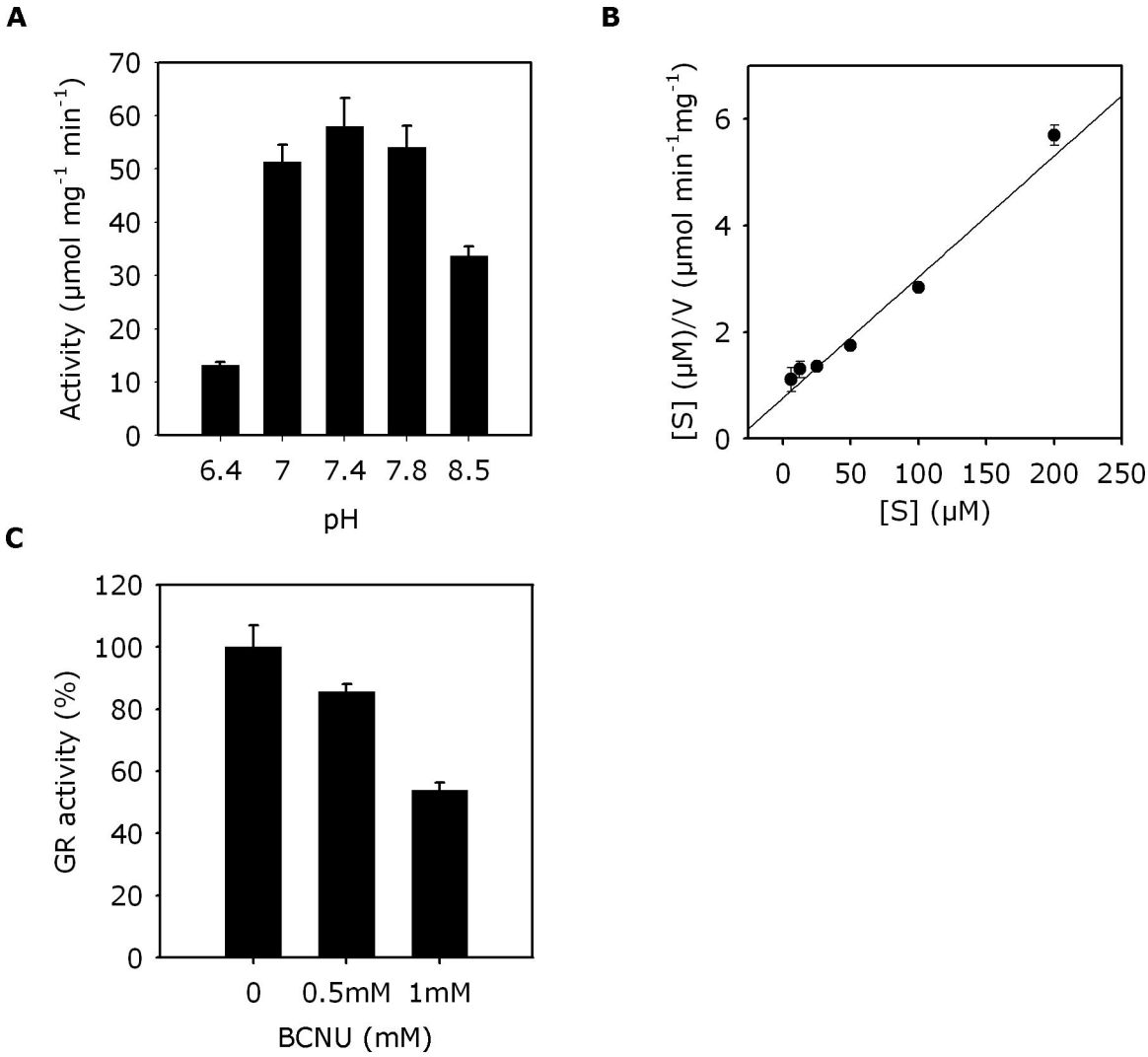

Fig. S2. Biochemical characterization of cytosolic glutathione reductase GR1. (*A*) pH dependence of GR1. Enzymatic assays were performed in sodium phosphate buffers at pH 6.4–8.5, highest activity was reached at pH 7.4. (*B*) Hanes plot for kinetic analysis of GR1 regarding the substrate NADPH. The enzyme assay was performed with 1 mM GSSG and 6.25–200 μM NADPH. All values are means ± SD ($n = 3$). $R^2 = 0.97$. (*C*) Inhibition of GR1 by 1,3-bis(2-chloroethyl)-1-nitrosourea (BCNU). BCNU was added to the assay to the indicated concentrations and the decrease in the initial velocity of GR1 was compared with the control. Means ± SD ($n = 3$).

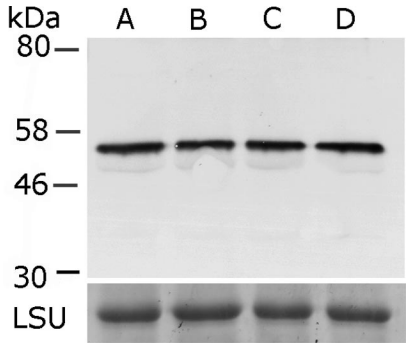

Fig. S3. Gel blot analysis of GR2 protein in different mutant backgrounds. Protein gel blot analysis with antiserum raised against GR2; 15 μg of total protein of Col-0 (*A*), *gr1-1* (*B*), *gr1-2* (*C*), and *ntra ntrb* double mutant (*D*) were separated on a 10% SDS/PAGE and electro blotted to nitrocellulose. Equal loading in is confirmed by staining of the large subunit (LSU) of 1,5-bisphosphate carboxylase/oxygenase (Rubisco).

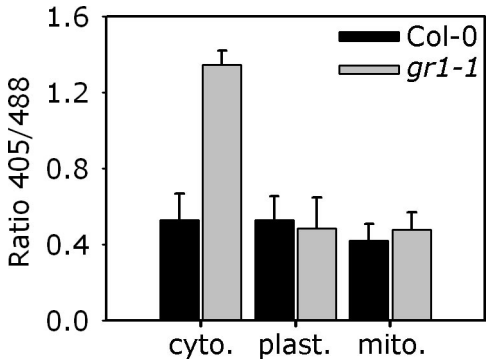

Fig. S4. Compartment-specific analysis of E_{GSH} in wild-type Col-0 and *gr1* plants. For measurement of cytosolic E_{GSH}, plants were transformed with GRX1-roGFP2. Measurements in plastid stroma and the mitochondrial matrix were done with free roGFP2. Images of seedling leaves were taken by CLSM with excitation at 405 and 488 nm, respectively. Data show means ± SD ($n = 5$).

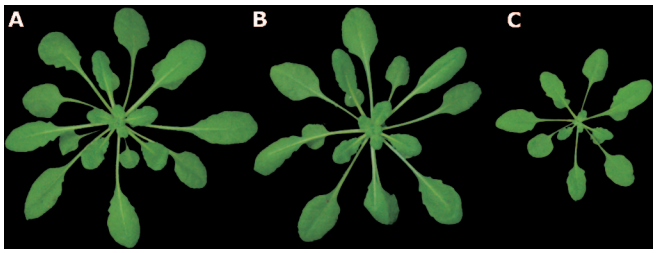

Fig. S5. Phenotypes of *gr1* and *ntra ntrb* deletion mutants. (*A*) Col-0, (*B*) *gr1-1*, and (*C*) *ntra ntrb* double mutant. All plants were 6 weeks old.

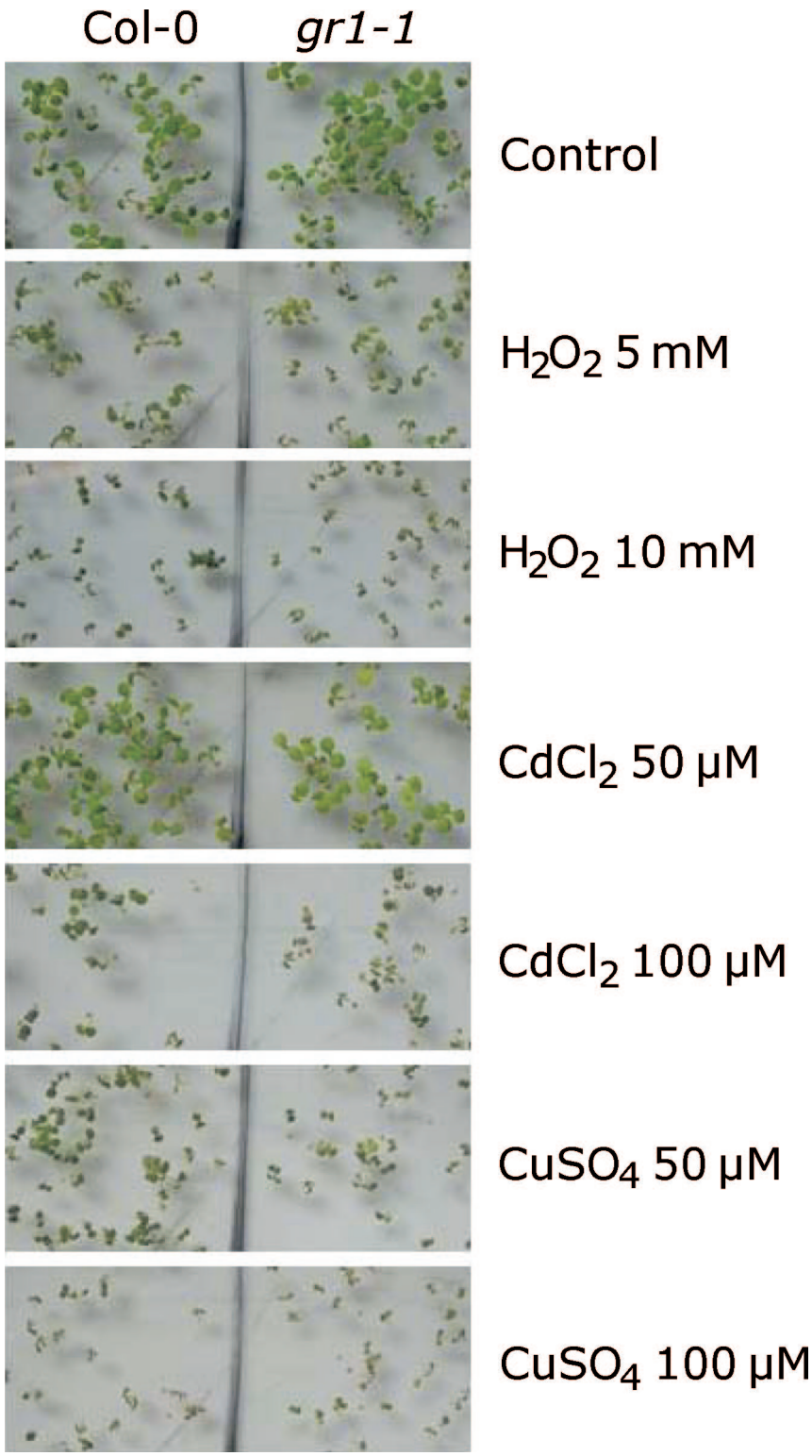

Fig. S6. Growth of wild-type (Col-0), and *gr1-1* mutant under stress conditions. Seeds were soaked on 0.5× MS agar plates supplemented or not (C) with different concentrations of H_2O_2, $CdCl_2$, and $CuSO_4$. Plants were grown under a 16-h light/8-h dark regime for 5 d.

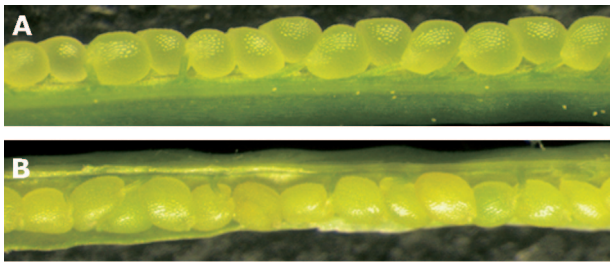

Fig. S7. Self-fertilization of *GR1/gr1-1 ntra ntrb* plants does not cause premature ovule abortion. (*A*) Col-0; (*B*) *GR1/gr1-1 ntra ntrb*. All seeds in siliques developing on a *GR1/gr1-1 ntra ntrb* show a wild-type phenotype. Lack of ovule abortion indicates that haploid ovules carrying mutant alleles for all 3 genes are still viable.

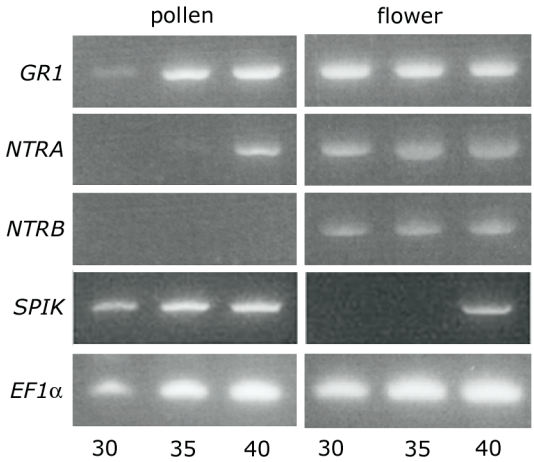

Fig. S8. Semi-quantitative RT-PCR was done on RNA extracted from mature pollen and mature flowers for 30, 35, and 40 cycles. *SPIK* was used as a pollen specific control gene. Note that the level of SPIK cDNA is almost saturating after 30 cycles in pollen. However, 40 cycles are required to detect SPIK cDNAs in flowers, because of the low ratio of pollen RNAs in flower RNAs.

Other Supporting Information Files

Table S1 (PDF)
Table S2 (PDF)